Epitaxial growth of $SrTiO_3$ on $SrTiO_3(001)$ using an oblique-incidence reflectance-difference technique

X. D. Zhu*
Department of Physics, University of California, Davis, California 95616-8677

H. B. Lu, Guo-Zhen Yang, Zhi-Yuan Li, Ben-Yuan Gu, and Dao-Zhong Zhang
Institute of Physics, Academic Sinica, P.O. Box 603, Beijing 100080, People's Republic of China
(Received 29 May 1997)

In a measurement of pulsed laser deposition of $SrTiO_3$ on $SrTiO_3(001)$, we demonstrate that the difference in *relative* reflectivity change $\Delta R/R$ between *s*- and *p*-polarized light can be used in a real-time monitor of thin film growth at the level of a single atomic layer. This reflectance difference has the same sensitivity (0.01 monolayer), the real-time monitoring capability, and the spectral resolution as the conventional reflectance-difference spectroscopy developed by Aspnes and co-workers. The present reflectance-difference technique does not rely on the existence of optical anisotropy within the surface plane and therefore is applicable to investigation and control of thin film growth on *all* surfaces. Compared to the surface photoabsorption technique developed by Kobayashi and Horikoshi, our technique improves the signal-to-noise ratio by at least one order of magnitude through reducing the background to a level equivalent to $\Delta R/R=1\times10^{-5}$ or below. [S0163-1829(98)01204-1]

The growth of artificial crystalline materials on a large scale through homoepitaxy and heteroepitaxy with full control over the composition and structure at the atomic level has become one of the most exciting areas of research in condensed matter physics and materials sciences. The ultimate goal is to fabricate new materials with the desired properties essentially by prescription. One of the crucial steps in the epitaxial growth of artificial materials is to monitor and in turn actively control the structure of the growing material. Optical techniques such as reflectance-difference spectroscopy (RDS),[1] surface photoabsorption near the Brewster angle,[2] and second-harmonic generation (SHG) spectroscopy[3,4] are generally suitable for such a purpose as they can be used as real-time, *in situ* probes that are effective even under nonultrahigh-vacuum conditions. In particular, reflectance-difference spectroscopy developed by Aspnes and co-workers has been successfully used in the investigation and optically controlled fabrication of the molecular beam epitaxy of III-V compounds and II-VI compounds.[1,5–10] In RDS, the difference between normal-incidence reflectance of light polarized parallel and perpendicular to a principal crystallographic axis in the plane of the surface is interrogated. It is particularly effective in monitoring the growth of thin films whose outermost layer has intrinsic or induced optical anisotropy within the surface plane. Aspnes and co-workers and others have demonstrated that RDS has sensitivity to the deposition of 0.01 monolayer adatoms.[1] By operating at appropriate optical wavelengths, RDS can be used as a monitor of either the surface structure [much like reflection high-energy electron diffraction (RHEED)] or surface chemical bonding.[5] Currently, RDS is being developed into an integral part of closed-loop control in the thin film growth process.[7,8] However, to extend the conventional RDS to growth surfaces that lack the in-plane optical anisotropy is problematic.

In the present paper, we demonstrate experimentally that a different form of reflectance-difference spectroscopy is equally effective for monitoring thin film growth regardless of whether or not the growth surface has in-plane optical anisotropy. We measure the difference between the reflectance of *s*- and *p*-polarized light at *oblique incidence*. It is well known that the reflectivities for *s*- and *p*-polarized light from a surface differ at oblique incidence and that the *difference is a function of the optical dielectric constant of the substrate*. In a surface process such as adsorption or nucleation and growth on a substrate, the chemical composition and structure in the outermost layer of the substrate change and the optical dielectric constant of the layer changes as well. We exploit the difference in the *relative* reflectivity change between *s*- and *p*-polarized light. The sensitivity and effectiveness of this technique do not rely on intrinsic or induced in-plane surface optical anisotropy. Consequently, the technique can be used to interrogate kinetic processes and reactions on *all* surfaces. Compared to the surface photoabsorption near Brewster angle where the bulk contribution is only reduced, this technique can eliminate the bulk contribution and thus further improves the signal-to-noise ratio and the sensitivity by at least one order of magnitude.[2,11] This capability is particularly significant in the investigation of substrates such as metals whose extinction coefficients are not negligible. Only in the transparent region of a substrate is the surface photoabsorption (SPA) directly proportional to the change in the outermost layer and thus has the same sensitivity as the present polarization reflectance-difference technique. A number of groups recently applied this form of polarization reflectance-difference spectroscopy to an investigation of adsorption, desorption, and surface diffusion of gaseous adsorbates on metals.[12–14] These authors have shown that the technique is sensitive to a relative reflectivity change $\Delta R/R=1\times10^{-5}$ and to a coverage change $\Delta\theta=0.02$. In this paper, we intend to show that it is also effective in monitoring the growth of crystalline thin films.

The optical measurement is performed on a laser molecular-beam-epitaxy system. The system is equipped

with a conventional reflection high-energy electron diffraction apparatus. We monitor the growth of $SrTiO_3$ on a $SrTiO_3$(001) by simultaneously measuring the *oblique-incidence* reflectance difference and the first-order RHEED intensity. A rectangular-shaped $SrTiO_3$(001) substrate (5 mm×10 mm×0.5 mm) is attached to a stainless-steel sample holder. The holder is heated from the back by a Ta filament. We attach a thermocouple to the sample holder for temperature control. The temperature of the $SrTiO_3$ substrate is calibrated with an optical pyrometer against that of the sample holder. The growth measurement is performed at a substrate temperature of around 920 K. As usual with laser molecular beam epitaxy of oxide materials, the deposition and growth chamber is filled with purified oxygen at a partial pressure of 2×10^{-4} Pa in order to maintain sufficient oxygen supply to the grown film. The base pressure is typically 5×10^{-8} Pa. At around 920 K, impurity gases in the ambient other than oxygen stay clear of the substrate surface.

For the RHEED measurement, an electron beam with an energy of 2.5×10^4 eV is incident on the $SrTiO_3$ substrate at an angle of $\theta_{\mathrm{RHEED}}=87°$.[15] The RHEED incidence plane coincides with the [010] axis of the substrate surface. We measure the intensity of the first-order diffraction with a charge-coupled-device (CCD) camera. For laser ablation deposition, we use a single-crystal plate of $SrTiO_3$ as the target. It is mounted in front of the $SrTiO_3$(001) substrate at a distance of 6.5 cm. We use the 308 nm optical pulses from a Lamda Physik LEXTRA 200XeCl excimer laser to irradiate the target. A single-pulse energy of 280 mJ is focused onto the target to yield an irradiation energy density of 1.0 J/cm^2. At this energy level, it takes 34 pulses to deposit one monolayer (ML) of $SrTiO_3$ as determined from the RHEED oscillation measurement.[16] By varying the repetition rate of the laser from 1 to 10 pulses per second, we can vary the averaged deposition rate from 0.03 to 0.3 ML/sec. During the deposition, the laser beam is scanned across the target surface to improve the homogeneity of the film growth over a large area on the substrate.

For the optical reflectance-difference measurement, we use a 0.34 mW, linearly polarized He-Ne laser operated at 6328 Å as the probe beam. The incidence angle of the probe beam is $\theta_{\mathrm{RDS}}=83°$ with the optical incidence plane coinciding with the [100] axis of the substrate surface. The index of refraction of $SrTiO_3$ single crystal at 6328 Å has been determined by McKee *et al.* to be 2.379.[17] A schematic sketch of the optical setup is shown in Fig. 1. The probe beam is initially *p* polarized. It first passes through a photoelastic modulator (PEM90, from Hinds Instruments, Inc.). The *p* polarization bisects the two principal axes of the modulator. The modulator produces a phase shift between the two components along the principal axes at a frequency of $\Omega=50$ kHz. The maximum phase shift is set at $\Phi=\pi$ or 180°. As a result, the polarization of the outgoing He-Ne laser beam is altered from *p* polarization to *s* polarization at a frequency of $\Omega=50$ kHz. The polarization-modulated beam then passes through a set of three fused quartz windows with their incidence planes overlapping with that of the substrate. These quartz windows can be tilted such that the transmittance of the *s*-polarized component can be reduced relative to that of the *p*-polarized component for reasons that will be clear shortly. The beam is then incident on the substrate. The

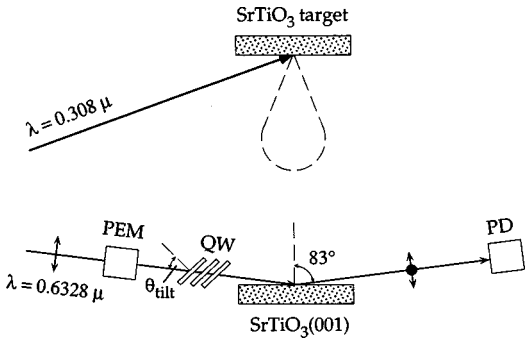

FIG. 1. Sketch of the experimental setup for the pulsed laser ablation deposition and the oblique-incidence reflectance-difference measurement. PEM: photoelastic modulator. QW: fused quartz parallel window. PD: biased silicon photodiode. The wavelength of the ablation laser is 0.308 μm or 308 nm. The wavelength of the probe laser is 0.6328 μm or 632.8 nm. Both the substrate and target are inside a thin film growth chamber.

reflected beam intensity is detected with a biased silicon photodiode (model 818-B8-40, from Newport-Klinger) and the photocurrent goes into a Stanford Research 510 lock-in amplifier with an averaging time constant of 0.3 sec. We monitor the ac component $I(2\Omega)$ of the reflected beam intensity at the second harmonics of the modulation frequency $\Omega=50$ kHz. The calculation shows that[1,13]

$$I(2\Omega)=\tfrac{1}{2}J_2(\Phi)I_{\mathrm{inc}}[|r_p(\theta_{\mathrm{RDS}})t_p(\theta_{\mathrm{tilt}})|^2 - |r_s(\theta_{\mathrm{RDS}})t_s(\theta_{\mathrm{tilt}})|^2]. \quad (1)$$

$r_p(\theta_{\mathrm{RDS}})$ and $r_s(\theta_{\mathrm{RDS}})$ are the reflectivities for *p*- and *s*-polarized light at the incidence angle θ_{RDS}. Here $t_p(\theta_{\mathrm{tilt}})$ and $t_s(\theta_{\mathrm{tilt}})$ are the total transmission coefficients for *p*- and *s*-polarized light through the fused quartz windows at a tilt angle θ_{tilt} (the incidence angle with respect to the quartz windows). $J_2(\Phi)$ is the Bessel function of the *second* kind and in our case $J_2(\pi)=0.486$. At oblique incidence, $r_s(\theta_{\mathrm{RDS}})$ is always larger than $r_p(\theta_{\mathrm{RDS}})$ in magnitude. The key of the present technique is that the contribution from the bulk substrate to the reflectance-difference signal can be eliminated by adjusting θ_{tilt} so that prior to a surface process the reflected intensities for *s* and *p* polarizations are equal, $|r_{p0}(\theta_{\mathrm{RDS}})t_p(\theta_{\mathrm{tilt}})|^2=|r_{s0}(\theta_{\mathrm{RDS}})t_s(\theta_{\mathrm{tilt}})|^2$. With essentially zero background, the subsequent change in the reflectance-difference signal comes only from the change in the outermost layer of the substrate,

$$I(2\Omega)\cong\tfrac{1}{2}J_2(\Phi)I_{\mathrm{inc}}|r_{p0}(\theta_{\mathrm{RDS}})t_p(\theta_{\mathrm{tilt}})|^2\left[\mathrm{Re}\left(\frac{r_p-r_{p0}}{r_{p0}}\right) - \mathrm{Re}\left(\frac{r_s-r_{s0}}{r_{s0}}\right)\right]. \quad (2)$$

It is proportional to the difference in the relative reflectivity change between *p*- and *s*-polarized light. Depending upon the specifics of the surface process in question, the reflectivity change can come from the simple addition of an overlayer with a distinctly different optical dielectric constant from the underlining substrate or a transformation of the outermost layer of the substrate by chemisorption of reactive adatoms.[13] In a homoepitaxy such as the growth of $SrTiO_3$

on $SrTiO_3(001)$, the reflectivity change comes from the structural and chemical bonding change in the outermost layer. If the growth proceeds three dimensionally such that the structure of the topmost layer changes irreversibly, the optical reflectance difference is also expected to change irreversibly. If, on the other hand, the epitaxy growth proceeds in a layer-by-layer mode such that the structure and chemical composition of the topmost layer changes periodically, we expect the reflectance difference to oscillate just as RHEED. It is this aspect of the oblique-incidence reflectance difference and its spectral tunability that will enable monitoring the growth mode and chemical properties of thin films. It is noteworthy that the setup shown in Fig. 1 appears to be similar to a conventional phase-modulated ellipsometry configuration without an analyzing polarizer.[18] The important difference is that the absence of an analyzing polarizer and the use of quartz windows to *nullify* the initial difference of the reflected intensities of *s*- and *p*-polarized components make the subsequent change in the reflectance difference *only* proportional to the change in the outermost layer of the substrate. Given a finite intensity fluctuation of the light source, the present technique in a simple way truly maximizes the sensitivity of an optical reflectance technique to submonolayer levels as demonstrated here and in Refs. 12–14. We should mention that it is possible to configure a phase-modulated ellipsometry by adding quartz windows as in the present study and a Pockel cell on the incidence side of the setup such that the initial differences in reflectance and phase between two polarizations are nullified. This was in part demonstrated by, for example, Hsiung and co-workers.[19] For the same sensitivity or signal-to-noise ratio, such a phase-modulated ellipsometry setup is much more involved and consequently expensive.

To establish the sensitivity of the oblique-incidence reflectance difference, we performed the measurement of the RHEED intensity and the reflectance difference simultaneously in a series of interrupted growth cycles of $SrTiO_3$ on $SrTiO_3(001)$ at $T=928$ K. In an interrupted growth cycle, the laser ablation is stopped, after the material equivalent of one monolayer is deposited, to allow for the growth surface to anneal. We use 34 ablation pulses to deposit one monolayer of $SrTiO_3$ at an averaged deposition rate of $R=0.09$ ML/sec. In Fig. 2, we display the results of these measurements in five consecutive growth cycles. The optical reflectance difference signal almost mirrors the change in the first-order RHEED intensity. From the RHEED intensity, it is clear that by allowing for the $SrTiO_3$ surface to recover for 50 sec at the growth temperature of 928 K, the surface morphology is restored to the same state as at the beginning of the deposition. As expected, the optical signal also recovers to the level prior to the deposition after an initial increase. The maximum change in the reflectance difference in terms of $\mathrm{Re}\{\Delta r_p/r_{p0}-\Delta r_s/r_{s0}\}$ is about 5×10^{-2}. The noise level, although not optimally reduced in our present measurement, is typically 2×10^{-3} as is shown in Fig. 2. It corresponds to a sensitivity to deposition of 0.04 ML in the present investigation. With further improvement of the mechanical stability of the optical setup, we expect to improve the sensitivity well below 0.01 ML. It is noteworthy that the RHEED intensity begins to recover before the deposition of one monolayer is completed, which indicates that local structure ordering has

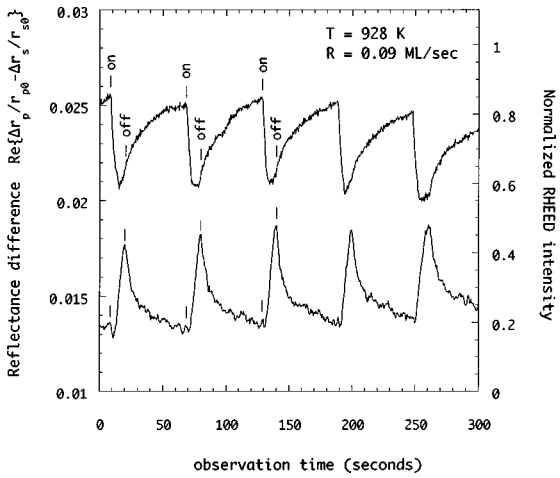

FIG. 2. Simultaneously measured reflectance-difference signal (lower curve) and the normalized first-order RHEED intensity (upper curve) vs time during five interrupted growth cycles. One monolayer of $SrTiO_3$ molecules is deposited in each cycle. The deposition rate is 0.09 ML/sec. The sample temperature is 928 K. On: ablation deposition starts. Off: ablation deposition stops.

begun to take place. In contrast, the reflectance difference continues to increase and starts to recover only when the deposition is completed and stopped. This is expected as the reflectance difference is not strictly probing the structural change of the outermost surface layer, but rather the resultant change in the averaged optical response of the layer.

We next use the reflectance-difference measurement to determine the growth mode at 920 K. In Fig. 3, we show the optical signals in a series of interrupted growth cycles during which we deposit one monolayer of $SrTiO_3$ in each of the first two growth cycles and then only half a monolayer in each of the following two cycles. The maximum change in the reflectance difference is almost one-half of what a monolayer deposition produces. Most importantly, the optical signal recovers to the level as at the beginning of the deposition.

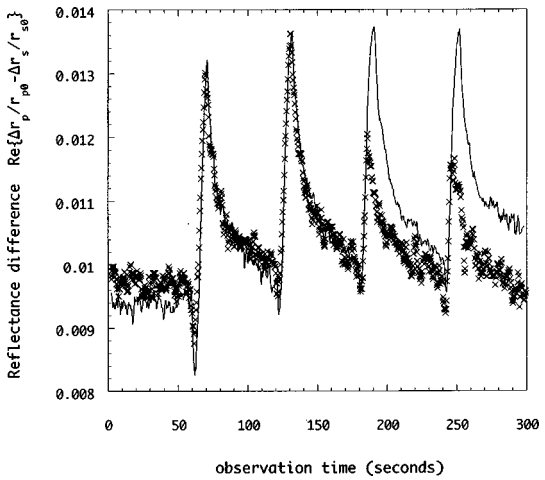

FIG. 3. Reflectance-difference signals vs time in four consecutive interrupted growth cycles. Solid curve: one monolayer of $SrTiO_3$ molecules is deposited in each cycle. Crosses: one monolayer of $SrTiO_3$ molecules is deposited in the first two cycles, and one-half of a monolayer of $SrTiO_3$ molecules is deposited in the last two cycles.

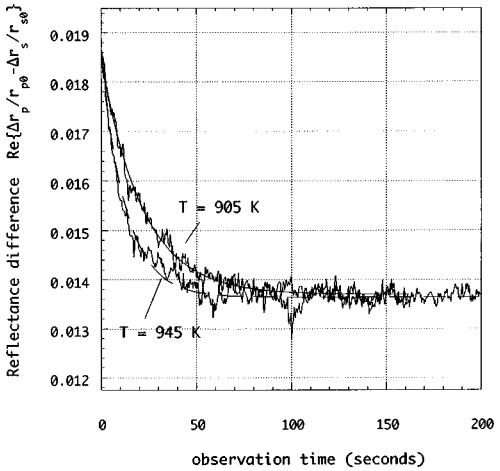

FIG. 4. Reflectance-difference signals during the recovery part of interrupted growths at two different temperatures. At 905 K, the decay time constant is $\alpha(T=905\ \mathrm{K})=0.047\ \mathrm{sec}^{-1}$. At 945 K, the decay time constant is $\alpha(T=945\ \mathrm{K})=0.09\ \mathrm{sec}^{-1}$.

This indicates that on a time scale of tens of seconds the growth of $SrTiO_3$ at 920 K proceeds in a step-flow mode rather than a nucleation-growth-coalescence mode on terraces. In the latter case, the deposition of half a monolayer would result in a surface morphology significantly different from that prior to deposition and in turn an incomplete recovery in the reflectance difference. We can therefore conclude that the recovery in the RHEED intensity and the reflectance difference records the breakup of small islands and the subsequent diffusion of monomers across terraces before being captured at terrace step edges.

From the rates of recovery, we are able to obtain an averaged thermal activation energy that characterizes the recovery. In Fig. 4, we show the reflectance-difference signals measured at 905 and 945 K after the deposition of one monolayer of $SrTiO_3$. The deposition rate is again $R=0.09$ ML/sec. The signals during the recovery are fit reasonably well to single-exponential functions. At $T=905$ K, the decay rate is $\alpha(T=905\ \mathrm{K})=0.047\ \mathrm{sec}^{-1}$. At $T=945$ K, the decay rate increases to $\alpha(T=945\ \mathrm{K})=0.09\ \mathrm{sec}^{-1}$. If we assume that the decay rate is dominated by only one kinetic process with a characteristic activation energy E_a (in units of kcal/mol) such that $\alpha(T)=\alpha_0\exp(-E_a/RT)$, we arrive at $E_a=26.5$ kcal/mol or 1.2 eV. Considering that the bonding of $SrTiO_3$ on $SrTiO_3$(001) is ionic, there are two possible candidates, either one of which can be the rate-limiting process. One is the surface diffusion of $SrTiO_3$ ''monomers'' across the width of a terrace. The other is the dissociation of small islands, particularly the evaporation of the edge molecules from these small islands on terraces. In the analysis that follows, we show that the surface diffusion of monomers is most likely the rate-limiting process in our case. Since our averaging time constant is 0.3 sec, we only monitor processes with characteristic time constants longer than 0.3 sec. Prior to our study, Chern and co-workers also performed an extensive RHEED study of $SrTiO_3$ growth on $SrTiO_3$(001) using pulsed laser deposition.[20] In their study, the substrate temperature during growth is $T_1=1023$ K. By sampling the RHEED intensity at a time interval of 50 msec, these authors observed a short recovery immediately after each pulse deposition with a time constant of about $\tau_1\approx150$ msec and a long recovery after the growth of a few molecular layers. The latter has a time constant of about 80 sec. As suggested by Chern and co-workers, the short recovery is likely the result of the reduction in the monomer density as the monomers diffuse towards relatively stable islands and terrace step edges or nucleate with other monomers. The process is completed when the monomer density reaches the equilibrium value on open terraces. The characteristic time is diffusion limited, $\tau\approx(L^2/D_0)\exp(E_{\mathrm{diff}}/RT)$, where L is the characteristic distance that monomers must traverse before being captured and D_0 is the diffusivity of monomers. If one assumes that $SrTiO_3$ dimers are stable over a time scale of 1 sec and are relatively immobile, the island density is roughly 1/3 of the deposited monomer density. In the study of Chern and co-workers, the islands density is estimated to be about 0.017 ML and the corresponding distance between two neighboring islands is roughly $L_1=30$ Å. On our $SrTiO_3$(001) sample, we determined with an atomic force microscope that the average terrace width is close to $L_2=150$ Å. Using an activation energy of 26.5 kcal/mol and a diffusion time $\tau_1\approx150$ msec in the study by Chern and co-workers, we estimate the surface diffusion time across a terrace of a width $L_2=150$ Å at $T_2=945$ K to be $\tau_2\approx\tau_1(L_2/L_1)^2\exp[E_{\mathrm{diff}}/RT_2-E_{\mathrm{diff}}/RT_1]=11$ sec. It corresponds to a recovery rate of $\alpha=0.09\ \mathrm{sec}^{-1}$, which agrees well with our experimentally observation of $\alpha(T=945\ \mathrm{K})=0.09\ \mathrm{sec}^{-1}$. It suggests that the recovery in our experiment is most likely to be rate limited by surface diffusion rather than the breaking up of small islands on terraces. A question remains as to why we did not observe the long recovery as observed by Chern and co-workers. We offer one possible explanation. In the study of Chern and co-workers, the recovery is after the deposition of many layers. It is known from the scanning tunneling microscopy (STM) and low-energy electron microscopy (LEEM) studies of the homoepitaxy of elemental metals that such a continuous deposition results in significantly more than two incomplete layers on the growth surface.[21–23] Consequently, the recovery is easily limited by the interlayer transport of monomers across the step edge rather than intralayer transport over flat terraces. An extra energy barrier (Schwoebel barrier) at a step edge can increase the recovery time by orders of magnitude. In our case only one monolayer is deposited in each growth cycle, and we expect only one incomplete layer on each terrace immediately after the deposition. As a result, the recovery in our experiment is expected to be limited only by the intralayer transport of monomers on flat terraces.

We now show that the overall reflectance-difference signal can be understood within the step-flow growth and diffusion-limited recovery model and a simplified model of the optical response of the outermost layer. In this simplified model, we assume that the optical reflectance difference mainly comes from the difference in the optical response between an edge atom and an atom embedded in the flat terrace so that $\mathrm{Re}\{\Delta r_p/r_{p0}-\Delta r_s/r_{s0}\}$ is proportional to the deviation of the mean coverage of the edge atoms from its equilibrium value $\langle\theta_{\mathrm{edge}}-\theta_{\mathrm{edge,equilibrium}}\rangle$. In a step-flow growth, the outermost surface layer consists of small islands and monomers on flat terraces. During the growth, the total number of surface atoms remains unchanged, while the num-

ber of the surface atoms at step edges (including monomers and those at the edges of small islands) changes. During deposition, the density of the edge atoms increases at the rate R. The increase is balanced by the loss of the edge atoms to capture at the edges of flat terraces. Thus the rate of loss is proportional to the diffusion constant D of monomers and the mean coverage of the edge atoms $\langle \theta_{\text{edge}} - \theta_{\text{edge,equilibrium}} \rangle$. We can write down the rate equation during the deposition,

$$\frac{d\langle \theta_{\text{edge}} - \theta_{\text{edge,equilibrium}} \rangle}{dt} = R - \gamma D \langle \theta_{\text{edge}} - \theta_{\text{edge,equilibrium}} \rangle, \tag{3}$$

and it is solved by $\langle \theta_{\text{edge}} - \theta_{\text{edge,equilibrium}} \rangle(t) = (R/\gamma D)[1 - \exp(-\gamma D t)]$. When the deposition is stopped, small islands on terraces begin to break up into monomers and the latter diffuse to the edges of the long terraces and become captured. This causes the density of edge atoms to drop to its equilibrium value at a rate

$$\frac{d\langle \theta_{\text{edge}} - \theta_{\text{edge,equilibrium}} \rangle}{dt} = -\gamma D \langle \theta_{\text{edge}} - \theta_{\text{edge,equilibrium}} \rangle, \tag{4}$$

and we find $\langle \theta_{\text{edge}} - \theta_{\text{edge,equilibrium}} \rangle(t) = \langle \theta_{\text{edge}} - \theta_{\text{edge,equilibrium}} \rangle(t=0)\exp(-\gamma D t)$. The optical reflectance difference is proportional to $\langle \theta_{\text{edge}} - \theta_{\text{edge,equilibrium}} \rangle$. The proportionality constant γ can be estimated as follows. We note that the averaged terrace width remains unchanged during the deposition and growth except that the step edges advance synchronously on the average. In the coordinate frame that rides with an advancing terrace edge, the deviation of the edge atom density, $\Delta\theta_{\text{edge}}(x,t) \equiv \theta_{\text{edge}}(x,t) - \theta_{\text{edge,equilibrium}}$, satisfies the one-dimensional diffusion equation with $\Delta\theta_{\text{edge}}(x,t)$ equal to zero at the terrace edges. The part of $\Delta\theta_{\text{edge}}(x,t)$ that dominates the long time recovery is its first Fourier component $\Delta\theta^{(1)}_{\text{edge}}(x,t) \equiv \Delta\theta^{(1)}_{\text{edge}}(L_t/2,0)\sin(\pi x/2L_t)\exp(-\pi^2 D t/4L_t^2)$. Thus the spatially averaged edge atom coverage varies with time as $\langle \theta_{\text{edge}} - \theta_{\text{edge,equilibrium}} \rangle(t) = \langle \theta_{\text{edge}} - \theta_{\text{edge,equilibrium}} \rangle(t=0)\exp(-\pi^2 D t/4L_t^2)$. Compared to Eq. (4), we arrive at $\gamma = \pi^2/4L_t^2$. From the recovery part of the reflectance-difference signal at $T = 945$ K, we find $\alpha(T = 945\text{ K}) = \gamma D = 0.09\ \text{sec}^{-1}$. Using $\alpha(T = 945\text{ K}) = \gamma D = 0.09\ \text{sec}^{-1}$ and the deposition rate $R = 0.1\ \text{sec}^{-1}$, we calculated $\langle \theta_{\text{edge}} - \theta_{\text{edge,equilibrium}} \rangle$ during the deposition of the interrupted growth cycle. In Fig. 5, we display the result of our model calculation together with the measurement at 945 K. The good agreement between the calculation and experiment indicates that simplified models of step-flow growth and the source of the reflectance difference adequately describe the physical situation in the present investigation.

We now discuss the results of our measurement and its potential application in active control of thin film growth. We have shown here that the oblique-incidence reflectance difference is sensitive to deposition of 0.04 ML of molecular adsorbates on a substrate surface. The sensitivity can be improved to deposition below 0.01 ML. Such a high sensitivity applies to the deposition and growth on metals as well as insulators[12,13,14]. In our present study where a He-Ne laser at a wavelength of 6328 Å is used, the reflectance-difference signal is mainly sensitive to the structural change and is shown to be an effective alternative to the RHEED intensity in monitoring the growth mode in the absence of a RHEED system or under conditions when a conventional RHEED cannot be operated. Since the reflectance difference measures the overall optical response of the outermost surface layer while the RHEED intensity measures the averaged structural ordering of the layer, the optical signal can complement the RHEED intensity measurement by offering a more detailed account of the evolution of a thin film growth, particularly during the growth of the initial few layers. For example, in an uninterrupted growth of $SrTiO_3$ on $SrTiO_3(001)$, we found that the reflectance difference only starts to oscillate after the deposition of three monolayers, while the RHEED intensity starts the oscillation cycles immediately after the deposition begins. This indicates that the surface morphology continues to evolve in a nonoscillatory fashion during the deposition of the first three monolayers. This observation is consistent with the STM images of homoepitaxy of elemental metals. Vrijmorth *et al.* and Esch *et al.* observed that in a damped layer-by-layer growth, the surface in fact builds up three or even more incomplete layers first before the morphology begins to change periodically[21,22]. Finally, we should be also able to monitor the chemistry during the thin film growth rather than the morphology by working at appropriate wavelengths similar to conventional RDS[1,5]. As the oblique-incidence reflectance-difference spectroscopy is applicable to surfaces with or without in-plane optical anisotropy and is inherently more sensitive than the surface photoabsorption technique, we fully expect our present technique will significantly expand the application of linear optical monitoring and control in thin film growths.

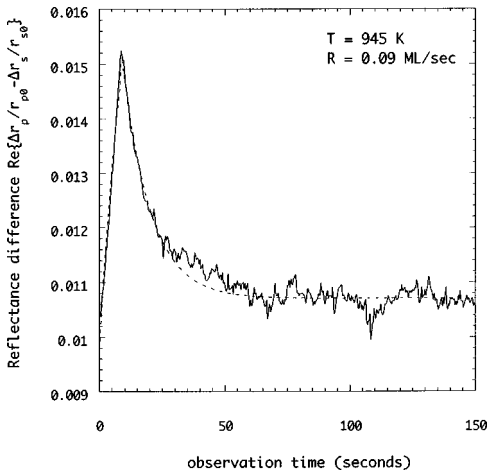

FIG. 5. Reflectance-difference signal (solid line) in a single interrupted growth cycle at $T = 945$ K. The dashed line is a fit to a step-flow growth that is rate limited by the diffusion of monomers across terraces. The optical reflectance-difference signal is assumed to be proportional to the deviation of the edge atom coverage from its equilibrium value (see text).

One of us (X.D.Z.) is grateful for the hospitality of the Institute of Physics, Academic Sinica. We thank Mao-Sen Yuan, Feng-Ying Miao, and Hua Wang for setting up the computer data acquisition and processing system used in this work. This work was in part supported by the National Science Foundation under Grant No. DMR-94-03441.

*Author to whom correspondence should be addressed. Electronic address: xdzhu@ucdphy.ucdavis.edu

[1] D. E. Aspnes, J. P. Harbison, A. A. Studna, and L. T. Florez, Phys. Rev. Lett. **59**, 1687 (1987); D. E. Aspnes, J. P. Harbiison, A. A. Studna, and L. T. Florez, J. Vac. Sci. Technol. A **6**, 1327 (1987); D. E. Aspnes, W. E. Quinn, and S. Gregory, *ibid.* **9**, 870 (1991).

[2] N. Kobayashi and Y. Horikoshi, Jpn. J. Appl. Phys., Part 1 **28**, L1880 (1989); **29**, L702 (1990); K. Nishi, A. Usi, and H. Sakaki, Appl. Phys. Lett. **61**, 31 (1992).

[3] T. F. Heinz, F. J. Himpsel, E. Palange, and E. Burstein, Phys. Rev. Lett. **63**, 644 (1989); S. S. Iyer, T. F. Heinz, and M. M. T. Loy, J. Vac. Sci. Technol. B **5**, 709 (1987).

[4] H. W. K. Tom, C. M. Mate, X. D. Zhu, J. E. Crowell, T. F. Heinz, G. A. Somorjai, and Y. R. Shen, Phys. Rev. Lett. **52**, 348 (1984).

[5] J. P. Harbison *et al.*, Appl. Phys. Lett. **52**, 2046 (1988); D. E. Aspnes, J. P. Harbison, A. A. Studna, and L. T. Florez, *ibid.* **52**, 957 (1988).

[6] D. E. Aspnes *et al.*, Phys. Rev. Lett. **61**, 2782 (1988).

[7] D. E. Aspnes, W. E. Quinn, M. C. Tamargo, and M. A. A. Pudensi, Appl. Phys. Lett. **60**, 1244 (1992).

[8] I. Kamiya, D. E. Aspnes, L. T. Florez, and J. P. Harbison, Phys. Rev. B **46**, 15 894 (1992).

[9] D. E. Aspnes, Surf. Sci. **307–309**, 1017 (1994).

[10] J. Jönsson *et al.*, J. Cryst. Growth **107**, 1047 (1991).

[11] K. Hingerl, D. E. Aspnes, I. Kamiya, and L. T. Florez, Appl. Phys. Lett. **63**, 885 (1993).

[12] X.-D. Xiao, Y. Xie, and Y. R. Shen, Surf. Sci. **271**, 295 (1992).

[13] A. Wong and X. D. Zhu, Appl. Phys. A: Solids Surf. **63**, 1 (1997).

[14] X. F. Jin, M. Y. Mao, S. Ko, and Y. R. Shen, Phys. Rev. B **54**, 7701 (1996).

[15] H. Koinuma and M. Yoshimoto, Appl. Surf. Sci. **75**, 308 (1994).

[16] Guo-zhen Yang, H. B. Lu, Wang Hui-sheng, Cui Da-fu, Yang Hai-qing, Wang Hua, Zhou Yue-Liang, and Chen Zheng-hao, Chin. Phys. Lett. **14**, 478 (1997).

[17] R. A. Mckee, F. J. Walker, E. D. Specht, G. E. Jellison, Jr., and L. A. Boatner, Phys. Rev. Lett. **72**, 2741 (1994).

[18] For example, B. Drevillon, Prog. Cryst. Growth Charact. Mater. **27**, 1 (1993).

[19] H. Hsiung, Th. Rasing, and Y. R. Shen, Phys. Rev. Lett. **57**, 3065 (1986); H. Hsiung, Ph.D. thesis, University of California at Berkeley, 1986.

[20] M. Y. Chern, A. Gupta, B. W. Hussey, and T. M. Shaw, J. Vac. Sci. Technol. A **11**, 637 (1993).

[21] J. Vrijmorth, H. A. van der Vegt, J. A. Meyer, E. Vlieg, and R. J. Behm, Phys. Rev. Lett. **72**, 3843 (1994).

[22] Stefanie Esch, M. Hohage, T. Michely, and G. Comsa, Phys. Rev. Lett. **72**, 518 (1994).

[23] J. Tersoff, A. W. Denier, and R. M. Tromp, Phys. Rev. Lett. **72**, 266 (1994).